

Automatic Removal of Externally Attached Fiducial Markers in Cone Beam C-arm CT

Martin Berger^{1,2}, Christoph Forman^{1,3}, Chris Schwemmer^{1,3}, Jang H. Choi⁴, Kerstin Müller^{1,3}, Andreas Maier¹, Joachim Hornegger¹, Rebecca Fahrig⁴

¹ Pattern Recognition Lab, Department of Computer Science, Friedrich-Alexander University Erlangen-Nuremberg, Erlangen, Germany

² Graduate School Heterogeneous Image Systems, Friedrich-Alexander University Erlangen-Nuremberg

³ Erlangen Graduate School in Advanced Optical Technologies (SAOT), Friedrich-Alexander University Erlangen-Nuremberg

⁴ Department of Radiology, Stanford University, Stanford, CA, USA



Introduction

Metallic markers are often used in CT to create accurate point correspondences, e.g. for registration or motion correction.

Prior to reconstruction markers are often removed from the projections to prevent streaking artefacts or to create ground truth data for the validation of marker-free processing methods [1].

In this work we compare six state-of-the-art removal techniques and their ability to restore edge, as well as noise properties.

Materials and Methods



1. Marker detection with fast radial symmetry transform [2]
2. Blank out detected markers in projections
3. Interpolate missing data by using surrounding, known data

Comparison of six different interpolation methods

LinInt: Linear interp. NConv: Normalised convolution [3]
 BSpl: B-Splines [1] SaS: Subtract-and-Shift [4]
 TPSpl: Thin-Plate-Splines Spec: Spectral interp. [5]

Experiments

Real data: C-arm CT dataset of left knee

8 externally attached markers at height of patella

Phantom: 3 cylinders modelling water, bone and bone marrow

8 markers attached in a helix at outer cylinder

- Reconstructions for each bead, centred around bead position
- Root mean square error (RMSE) computation for phantom data

Detector:	1240 x 960 pixels	Pixel spacing:	308 x 308 μm^2
Source-patient dist.:	785 mm	Source-detector dist.:	1199 mm
Scan range:	200°	No. of projections:	496
Reconstruction size:	256 x 256 x 256	No. of beads:	8
Voxel size:	125 x 125 x 125 μm^3	No. of removal steps:	3968

Results and Discussion

- Spec yielded best qualitative and quantitative results (cf. Figure 1h and Figure 2h)
- Spline-based approaches have reduced accuracy for real data (cf. Figure 1c,d and Figure 2c,d)
- LinInt properly removed markers but blurred edges (cf. Figure 1b and Figure 2b)
- NConv and SaS could not remove markers completely (cf. Figure 1f,g and Figure 2f,g)

[HU]	None	LinInt	BSpl	TPSpl	NConv	SaS	Spec
RMSE	30.12	13.84	9.26	9.91	19.50	14.62	8.08
σ_{rmse}	4.36	4.48	4.27	4.35	6.46	4.33	3.31

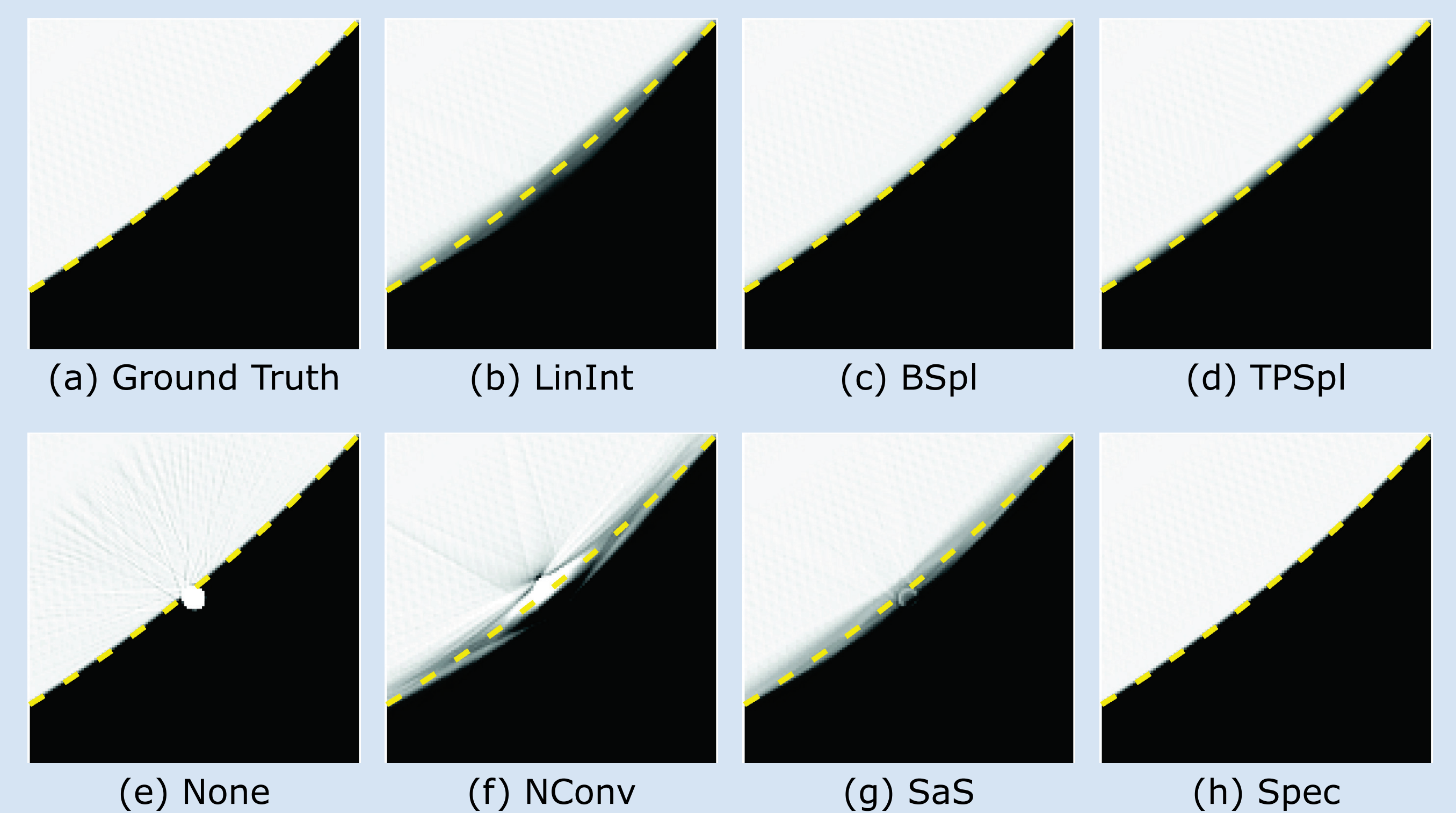


Figure 1: Marker removal results for the phantom data. The images show a 16 x 16 mm² region centred around a marker. The ground truth is shown in (a) and the reconstruction without marker removal in (e). The dashed, yellow line depicts the true cylinder edge. The display window was [-922, 51] HU.

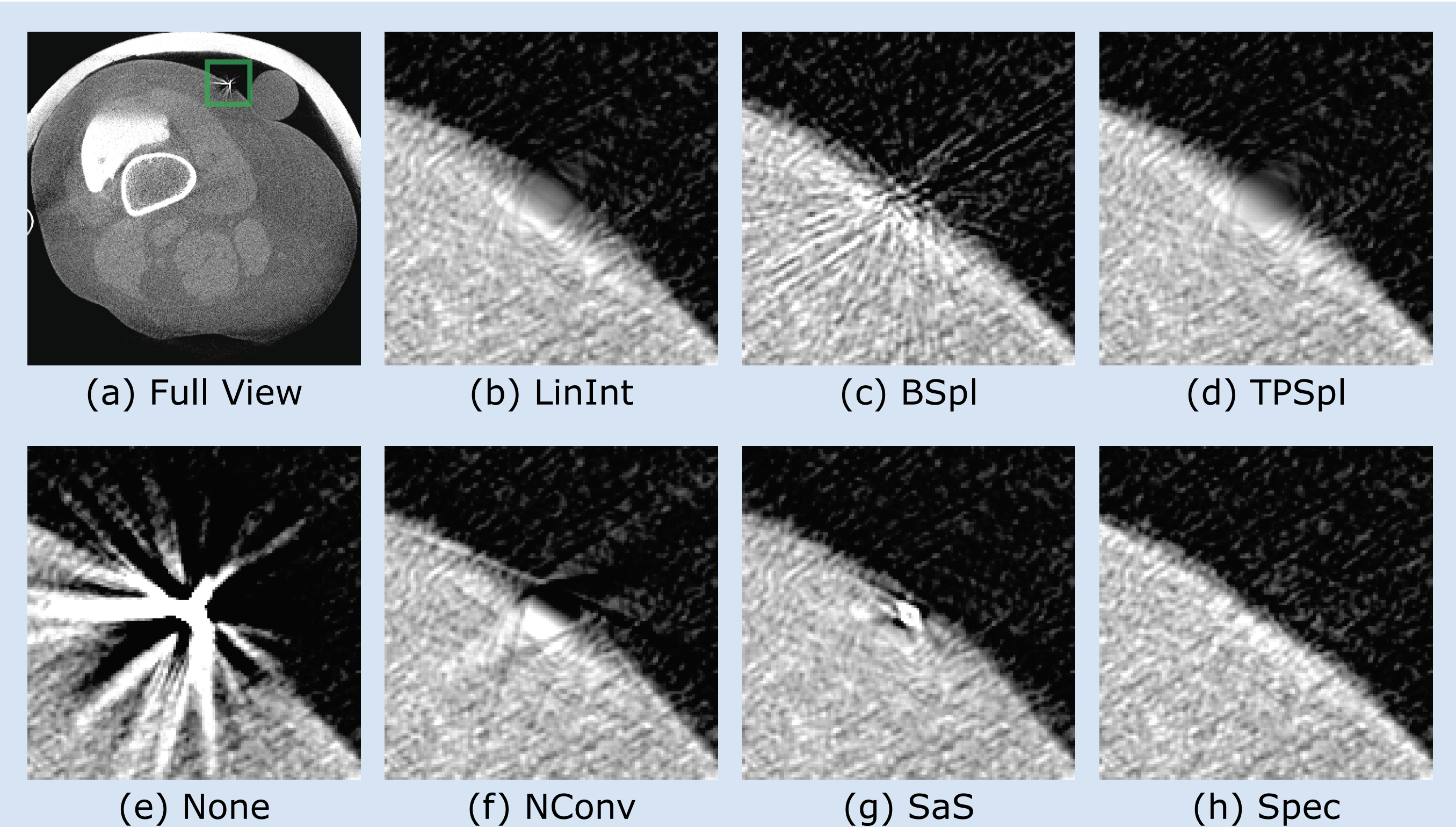


Figure 2: Reconstruction results for the real C-arm CT data after applying the different interpolation methods to the projections. The full slice is shown in (a) and the reconstruction without marker removal in (e).

Conclusions

- We compared six techniques for the removal of high-density fiducial markers from CT projection data
- The marker detection step is fully automatic using a fast radial symmetry-based approach
- Spectral interpolation performed best on our data, showing promising results in terms of edge and noise restoration
- An extension to arbitrary shaped markers is one objective for future work

References

- [1] Mitrovic et al. 3D-2D Registration of Cerebral Angiograms: A Method and Evaluation on Clinical Images. *Medical Imaging, IEEE Transactions on*. 2013;32(8):1550–1563.
- [2] Loy et al. Fast radial symmetry for detecting points of interest. *Pattern Analysis and Machine Intelligence, IEEE Transactions on*. 2003;25(8):959–973.
- [3] Knutsson et al. Normalized and Differential Convolution: Methods for Interpolation and Filtering of Incomplete and Uncertain data. *Proc. of Computer Vision and Pattern Recognition ('93)*; 1993. p. 515–523.
- [4] Schwemmer et al. High-Density Object Removal from Projection Images using Low-Frequency-Based Object Masking. *BVM 2010*. p. 365–369.
- [5] Aach et al. Defect interpolation in digital radiography: how objectoriented transform coding helps. *Proc. SPIE*. vol. 4322; 2001. p. 824–835.

Contact

✉ martin.berger@cs.fau.de
 🌐 <http://www5.cs.fau.de/~berger>



The authors gratefully acknowledge funding of the Erlangen Graduate School in Advanced Optical Technologies (SAOT) by the German Research Foundation (DFG) in the framework of the German excellence initiative and by the Research Training Group 1773 "Heterogeneous Image Systems", funded by the German Research Foundation (DFG).